Multiscale Gradient Maps Augmented Fisher Information-Based Image Edge Detection

V. B. SURYA PRASATH [1,2,3,4], **DANG NGOC HOANG THANH** [5], **NGUYEN QUOC HUNG** [5], **AND LE MINH HIEU** [6]

[1]Division of Biomedical Informatics, Cincinnati Children's Hospital Medical Center, Cincinnati, OH 45267, USA
[2]Department of Pediatrics, University of Cincinnati, Cincinnati, OH 45267, USA
[3]Department of Biomedical Informatics, College of Medicine, University of Cincinnati, Cincinnati, OH 45267, USA
[4]Department of Electrical Engineering and Computer Science, University of Cincinnati, Cincinnati, OH 45267, USA
[5]Department of Information Technology, School of Business Information Technology, University of Economics Ho Chi Minh City, Ho Chi Minh City 70000, Vietnam
[6]Department of Economics, University of Economics–The University of Danang, Da Nang 550000, Vietnam

Corresponding author: Dang Ngoc Hoang Thanh (thanhdnh@ueh.edu.vn)

ABSTRACT Image edge detection is an important task in image processing and pattern recognition. Edges in digital images signify image discontinuities and traditionally gradient information is utilized in finding possible edge pixels. In this work, we consider a fusion approach using multiscale gradient maps along with non-parametric Fisher information which is recently used in edge detection. By using multiscale gradient maps we obtain better edge localization and robust edge maps and local thresholding with Fisher information helps obtain better detection. Experimental results on a variety of digital images and performance evaluation undertaken in comparison with edge detectors from the literature show the advantage of the proposed approach.

INDEX TERMS Edge detection, image thresholding, fisher information, histogram, multiscale gradients, information theory.

I. INTRODUCTION

Edge detection is an integral part in various image processing, computer vision, and pattern recognition tasks. Edges visually represent image discontinuities whereby object boundaries can be discerned. Automatic edge detection is an important research area which is still open. Majority of the automatic image edge detection methods rely on derivatives and gradients [5]–[7] and one of the important detector is that of Canny [2]. These rely on gradient maps or smoothed gradient maps in locating image discontinuities to discern edge locations.

In recent years, there are several approaches were applied to solve the edge detection problem. Shi *et al.* [9] developed a novel hybrid edge detection method for polarimetric SAR images by fusing two kinds of edges: improved polarimetric constant false alarm rate edge detector and weighted gradient-based edge detector. Yahya *et al.* [12] proposed a novel edge detection method based on anisotropic diffusion and total variation models. Li *et al.* proposed an edge

detection method based on multiscale anisotropic Gaussian kernels [13]. Dagar *et al.* [18] used a binary particle swarm optimization to solve the edge detection problem. Another well-known edge detection method based on the modified Mumford-Shah model was proposed by Shi *et al.* [19]. The interpolation technique is also used such as an edge detection method based on radial basis function (RBF) interpolation [23]. Zotin *et al.* [26] proposed an edge detection method based on a fuzzy C-means clustering. Soft computing models such as type-2 fuzzy logic models have successfully been applied for edge detection [29], [22], [24]. Some other related edge detection methods have been considered in the past [16], [17], [21], [25].

Entropy theory is an important approach that is widely used for solving the edge detection problem: Zhen *et al.* [11] combined grey entropy theory and textural features to detect the edge, Sert and Avci [20] used a technique that is called a neutrosophy based on maximum norm entropy. Recently, Abdel-Azim *et al.* [1] proposed an edge detection algorithm based on non-parametric Fisher information (FI) measure [3], [4] based local thresholding value selection and masks. Promising results were obtained on edge detection of

---

The associate editor coordinating the review of this manuscript and approving it for publication was Hossein Rahmani [ID].

natural images when compared to edge detectors from the past. This method however suffers from the lack gradient information with low contrast edges are not captured and performs poorly when there is noise in images.

In this work, we propose a new edge detection by fusing multiscale gradient maps along with FI (MSFI) measure for improved detection results. We compared our method with the original FI [1], and other gradient based edge detectors such as Canny [2], Sobel [7], Prewitt [5], and Roberts [6] methods. Experimental results on a variety of natural images indicate that our approach obtains better edge detection results. Experimental results on a variety of images, synthetic, and natural images indicate that our MSFI based edge detector obtains competitive accuracy among the related models from the literature.

Rest of the paper is organized as follows. Section II studies the non-parametric Fisher information measure for edge detection with multiscale gradients fusion. Section III provides detailed experimental results on digital images and compares with other edge detectors from the literature. Finally, Section IV concludes the paper.

II. GRADIENT FUSED NON-PARAMETRIC FISHER INFORMATION MEASURE FOR EDGE DETECTION

A. FISHER INFORMATION

Fisher information (FI) is a non-parametric measure and though it is related to the Shannon entropy it predates it. Let Y be a discrete random variable, and characterized by the probability density function (PDF) $f_j, j \in N$ where N is the values taken by Y. The f_j, the probability of $y_j \in (a, b) \subset \mathbb{R}$, is normalized $\sum_{j=1}^{N} f_j = 1$. Hence, $Y = \{y_1, y_2, \ldots, y_N\}$ is specified by a probability vector $f = \{f_1, f_2, \ldots, f_N\}$. The FI measure is then given by,

$$I(Y) = \sum_j \frac{(f(y_{i+1}) - f(y_j))^2}{f(y_j)}. \tag{1}$$

Note that the Shannon entropy is defined as $H(Y) = -\sum_j f(y_j) \log f(y_j)$, however the FI has better sensitivity than the Shannon entropy to the density differences of the adjacent points of the variable. We now briefly recall the basic definitions and the FI measure based edge detector approach from [1].

Given a grayscale image I with gray levels $[0, 1, \ldots, L - 1]$, let the number of pixels with gray level j be n_j. The probability of gray level in the image is given by,

$$f_j = \frac{n_j}{N}, \quad f_j \geq 0, \quad \sum_{j=0}^{L-1} f_j = 1. \tag{2}$$

Abdel-Azim *et al.* [1] utilized the non-parametric FI measure to select a local threshold value. This value is then used to obtain a binary segmented image with foreground/object (*A*), and the remaining background (*B*). The edges were then detected using usual masks 3×3. The two probabilities of the

Algorithm 1 MSFI - Edge Detection by **M**ulti**S**cale **F**isher **I**nformation

---

Input: A grayscale image I of size $M \times N$, and $[\sigma_{low}, \sigma_{high}]$.
Output: Returns a binary edge image E of size $M \times N$.

1: **procedure** MSFI(I, σ_{low}, σ_{high})
2: **Begin**
3:    Compute the multiscale gradient maps, See Eqn. (10).
4:    Fuse the image and multiscale gradient maps, See Eqn. (11).
5:    Create a binary image using non-parametric Fisher information measure thresholding, See Eqn. (7)(8).
6:    For $1 \leq i \leq M$ and $1 \leq j \leq N$:
7:       Set $E(i, j) = I(i, j)$.
8:    For all $2 \leq j \leq N - 1$ and $2 \leq i \leq M - 1$.
9:       Set $sum = 0$;
10:      For all $-1 \leq k \leq 1$ and $-1 \leq l \leq 1$:
11:         If ($I(i, j) = I(i + k, j + l)$) Then
12:           Increase $sum = sum + 1$.
13:       If ($sum \leq 6$) Then
14:         Set $E(i, j) = 1$
15:      Else
16:         Set $E(i, j) = 0$.
17: **End**

---

two categories can be written as,

$$f_A = \frac{f_1}{w_1}, \frac{f_2}{w_1}, \ldots, \frac{f_t}{w_1}, \tag{3}$$

$$f_B = \frac{f_{t+1}}{w_2}, \frac{f_{t+2}}{w_2}, \ldots, \frac{f_{L-1}}{w_2}, \tag{4}$$

where $w_1(t) = \sum_{j=0}^{t} f_j$, and $w_2(t) = 1 - w_1(t)$ with luminance level t. The priori FI for each of these categories is then given as,

$$I_A(t) = \frac{1}{w_1} \sum_{i=0}^{t} \frac{(f(x_{i+1}) - f(x_i))^2}{f(x_i)}, \tag{5}$$

$$I_B(t) = \frac{1}{w_2} \sum_{i=t+1}^{L} \frac{(f(x_{i+1}) - f(x_i))^2}{f(x_i)}, \tag{6}$$

respectively with $x_i \in (a, b) \subset \mathbb{R}$. The FI measure of two classes is,

$$I(t) = w_1 I_A(t) + (1 - w_2) I_B(t). \tag{7}$$

The Fisher Measure Thresholding Algorithm (FIMTHA) is based determining the optimal threshold by maximizing the FI measure Eqn. (7),

$$t_{opt} = argmax_t \{I(t)\}. \tag{8}$$

From this binary image, the usual masks of size 3×3 are applied to obtain the final edge detection outputs.

B. MULTISCALE GRADIENT FUSION WITH FISHER INFORMATION

Though the FI measure based threshold and edge detector methods in general works well, when the images contain
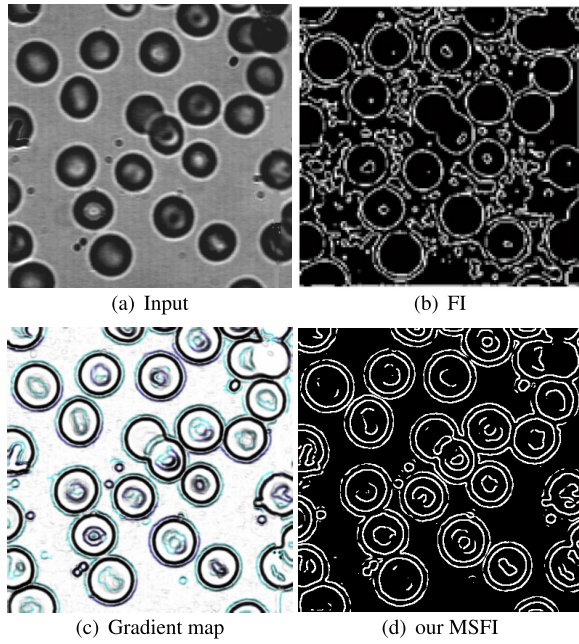
(a) Input	(b) FI
(c) Gradient map	(d) our MSFI

FIGURE 1. Multiscale gradient fusion helps improve the edge detection results in Fisher information measure approach. We show the gray scale Microscopy (B) image of size 380 × 390. (a) Input, (b) edges detected with FI [1], (c) multiscale gradients $[\sigma_{low}, \sigma_{high}] = [1, 3]$ based map $G(I)$ shown as a color image with channels ($|\nabla_\sigma I|, |\nabla_\sigma I|, |\nabla_\sigma I|$), (e) and edges detected with our multiscale Fisher information (MSFI) approach. The proposed MSFI obtains better edge detections and less spurious edge pixels by using augmenting multiscale gradient maps.

non-homogeneous grayscale variation the edge pixels can be missed and spurious pixels can be introduced due to the sensitivity of FI measure. To show this observation visually, we show in Figure 1(a) a gray scale Light microscopy (B) test image, and Figure 1(b) FI measure based edge detection result. To avoid this, in this work we introduce the pre-smoothed multiscale gradient maps, Figure 1(c), fused with the FI measure approach that obtains improved accuracy as shown in the result in Figure 1(d). Derivative information from gradient of a given image $\nabla I = (I_i, I_j)$ $(i, j) \in \Omega$ ($\Omega \subset \mathbb{R}^2$ the image domain) contain valuable information regarding image discontinuities. However, due to inherent noise in digital images, computation of gradients are influenced by noisy oscillations. To avoid this, gradient based edge detectors employ typically a pre-smoothing step e.g. with a Gaussian kernel [8], [31]. The smoothed gradient is given by,

$$\nabla_\sigma I = G_\sigma \star \nabla I(i, j), \qquad (9)$$

where $G_\sigma(i, j) = (\sigma\sqrt{2\pi})^{-1} \exp\left(-(i^2 + j^2)/2\sigma^2\right)$ is the 2D Gaussian kernel, $\star$ denotes the convolution operator, and $\sigma > 0$ is the standard deviation of the Gaussian distribution. The magnitude of the smoothed gradient map can give indication of where edges are in the image. However, a single scale value σ may not capture objects with different scales. One can use multiple scales to better retain objects of different scales within a single unified map,

$$G(I) = \cup_{\sigma=\sigma_{low}}^{\sigma_{high}} |\nabla_\sigma I|. \qquad (10)$$

The discrete interval $[\sigma_{low}, \sigma_{high}]$ captures a range of scales, that can be fixed based on the data set at hand, to retain edge maps across multiscale objects that are present in the image I. The presmoothing operation (9) mitigates the effect of noise on each gradient map, and the aggregation (10) makes sure the information from gradients are maximally utilized in the edge detection procedure. Such a fusion multiscale gradient maps is useful in capturing spatial gradient changes and can aid in improving the information content overall [28] We thus utilize the summed up gradient maps along with gray scale values and apply the FI measure based thresholded value selection for this combined image,

$$\mathbf{I} = I \cup G(I). \qquad (11)$$

Then, the usual masks are utilized to detect the edges. We term this approach as the multiscale Fisher information (MSFI) based edge detector, see the steps in algorithm 1. Figure 1 illustrates the advantage of using the multiscale gradient maps Figure 1(c), as can be seen in Figure 1(d) our improved method obtains overall a better edge map.

III. EXPERIMENTAL RESULTS
A. SETUP, PARAMETERS AND ERROR METRICS
We have implemented all the edge detectors considered here in MATLAB® R2012a on a Mac Laptop with 2.3 GHz Intel Core i7 with 8 GB RAM. All the images are mapped to [0, 1] and the edge maps are inverted (white - edge pixels, black - non-edge pixels) for better visualization. The computation of the overall MSFI took ∼ 0.2s on a 512×512 gray scale image. To test the performance of different edge detection algorithms quantitatively we utilize the following two error metrics.

- Entropy:

$$E(I) = -\sum_{i=0}^{L} p_i \log p_i, \qquad (12)$$

where p_i is the frequency of pixels with intensity value i. Low values of $E(I)$ indicate lower information and the higher values are indicative of noise and possible presence of double edge pixels.

- Pratt's figure of merit (FoM) [27]:

$$FOM = \frac{1}{\max(N_I, N_D)} \sum_{i=1}^{N_D} \frac{1}{1 + \gamma\, d_i^2}, \qquad (13)$$

where N_I, N_D represent the number of ideal and detected edge pixels, and d_i is the Euclidean distance between them. The parameter γ is used to penalize displacement of edge pixels from true locations. FoM values in the interval [0, 1] with values of FoM closer to 1 indicate better edge detector performance.

We further compare the peak signal to noise ratio (PSNR - dB) [30], [32].

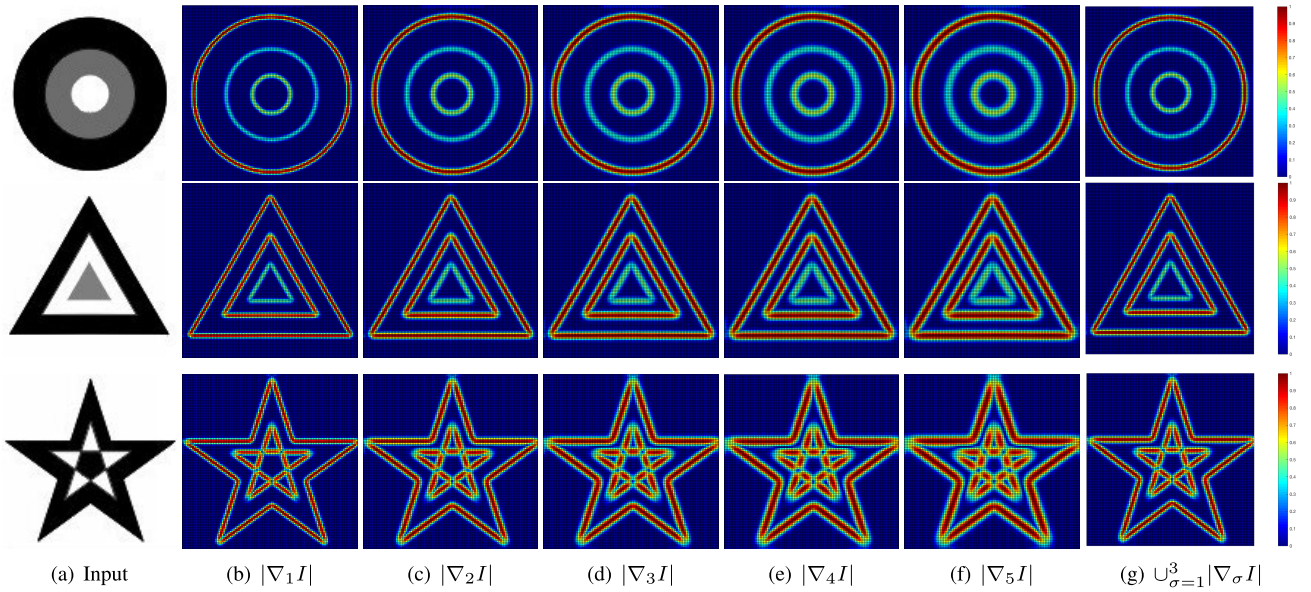$$PSNR(u) = 20 * \log_{10}\left(\frac{u_{max}}{\sqrt{MSE}}\right) dB \qquad (14)$$

FIGURE 2. Capturing multiscale edges via gradient maps augmentation on a synthetic Shapes gray scale image of size 512 × 512. We show different structures to illustrate the multiscale scales structures that are present in the image. (a) Input image, (b-f) smoothed gradient edge maps with $\sigma = 1, 2, 3, 4, 5$ shown as pixelmaps. Higher scales tend to obtain bigger edge map widths, and (g) $\cup_{\sigma=1}^{3}|\nabla_\sigma I|$, wherein we combined edge maps of $\sigma = 1, 2, 3$ to keeps all the salient structures intact without compromising the edge quality. Better viewed online and zoomed in.

TABLE 1. Comparison of PSNR (dB) values for Fisher information (FI) [1], Sobel [7], Canny [2], Prewitt [5], Roberts [6] detectors, and our multiscale Fisher information (MSFI).

Image	Fisher	Sobel	Canny	Prewitt	Roberts	Our MSFI
Light microscopy (A)	25.9744	25.9723	25.9738	25.9723	25.9722	25.9767
Light microscopy (B)	26.7263	26.7221	26.7229	26.7221	26.7224	26.7312
Lena	26.9582	26.9568	26.9579	26.9568	26.9569	26.9677
Cameraman	26.8964	26.8956	26.8967	26.8956	26.8959	26.9015
Leaf	26.6129	26.6126	26.6134	26.6126	26.6127	26.6228
Brain	29.2696	29.2671	29.2693	29.2670	29.2671	29.2684
Horse	25.8392	25.8366	25.8382	29.2670	25.8365	25.8456
Electric Circuit	28.1381	28.1365	28.1386	28.1365	28.1364	28.2204
Peppers	26.9156	26.9146	26.9156	26.9146	26.9145	26.9189
Grape	27.7102	27.7083	27.7105	27.7083	27.7082	27.7191

where MSE $= (mn)^{-1}\sum\sum(u - u_O)^2$, with u_O is the original (noise free) image, $m \times n$ denotes the image size, u_{max} denotes the maximum value, for example in 8-bit images $u_{max} = 255$. A difference of 0.5 dB can be identified visually. Note that the metric PSNR is meant for evaluating image quality and not for evaluating the accuracy of edge detection methods. However, in [1] PSNR (dB) was used to measure the better-thresholded image quality. They considered the edge detection based on threshold image values to make quantitative comparisons with PSNR values among different methods.

Following [1], we utilize 3×3 masks as in the FIMTHA model. For the range of scales used in our multiscale gradient maps augmentation (10), we conducted a parameter sweep. Figure 2 shows the multiscale gradient edge maps for various shapes from a synthetic gray scale image. These contain low, medium, and high scales, and the augmentation of multiscale gradient maps provides better edge localization and can preserve details at all scales, see for example, Figure 2 last row which contain small triangles as well the bigger star

shape. We fixed $[\sigma_{low}, \sigma_{high}] = [1, 3]$ as the optimal range for natural images considered here since higher scales tend to increase the edge map widths and can lead false edge pixels thereby degrading the accuracy. Further, by augmenting multiple scales based gradient maps augmented with the gray scale values as in (11) we obtain stronger responses by reinforcing real edge pixels on the boundaries of the shapes, see Figure 2 last column.

B. COMPARISON RESULTS
Figure 3 shows a comparison of our proposed MSFI with other edge detectors from the literature, Fisher information (FI) [1], Sobel [7], Canny [2], Prewitt [5], and Roberts [6]. Table 1 shows the corresponding PSNR (dB) values for the edge detection results. As can be seen, overall the proposed MSFI edge detection results are better. There are no pre- or post-processing steps applied to any of the experimental results reported here. We notice a lack of edge continuity, see for example in the images - Brain, Grape, and Lena top of the cap region, this is due to the fact that the augmented

(a) Input   (b) Sobel [7]   (c) Canny [2]   (d) Prewitt [5]   (e) Roberts [6]   (f) FI [1]   (g) our MSFI

FIGURE 3. Comparison of edge detection results on a synthetic *Shapes* image. (a) Input, (b) Sobel [7], (c) Canny [2], (d) Prewitt [5], (e) Roberts [6], (f) FI [1], and (g) our MSFI.

multiscale gradient maps can obtain lower values due to small scale oscillation compared to the uniform background pixels. A remedy to this can be to augment other differential operators such as the structure tensor [10], [14] or higher order derivatives.

Table 2 shows the Entropy and Pratt's figure of merit (FoM) metric for the test images considered here. As we can see, our model obtained better values of FoM than other edge detection methods indicating better edge pixels detection overall. Regarding the Entropy values, we notice that Sobel,

TABLE 2. Comparison of Entropy, and Pratt's figure-of-merit (FoM) values for Fisher information (FI) [1], Sobel [7], Canny [2], Prewitt [5], Roberts [6] detectors, and our multiscale Fisher information (MSFI).

Image	Fisher	Sobel	Canny	Prewitt	Roberts	Our MSFI
Light microscopy (A)	0.4024	0.03452	0.4088	0.3422	0.01241	0.4103
	0.5245	0.135	0.5814	0.1045	0.0912	0.6713
Light microscopy (B)	0.4322	0.1882	0.3578	0.1878	0.1856	0.4019
	0.7811	0.6209	0.7912	0.6218	0.6294	0.8005
Lena	0.3011	0.2046	0.4084	0.2378	0.2031	0.3281
	0.5917	0.2494	0.7816	0.2339	0.2142	0.8067
Cameraman	0.1897	0.2339	0.4287	0.2344	0.2759	0.3884
	0.5293	0.7844	0.8260	0.7669	0.7728	0.8562
Leaf	0.3460	0.2897	0.4275	0.2880	0.2743	0.3781
	0.5208	0.5281	0.7923	0.4885	0.4804	0.8102
Brain	0.3449	0.2301	0.4721	0.2296	0.2123	0.3562
	0.5098	0.4997	0.6179	0.4885	0.4228	0.5188
Horse	0.4871	0.2208	0.6718	0.2198	0.2179	0.5214
	0.5827	0.2345	0.768	0.2317	0.2300	0.6552
Electric Circuit	0.4629	0.3103	0.6018	0.3205	0.3001	0.5187
	0.7722	0.6208	0.7787	0.5178	0.4987	0.8110
Peppers	0.4912	0.2986	0.5993	0.2897	0.2944	0.5578
	0.4670	0.2143	0.7349	0.2104	0.2186	0.8754
Grape	0.3291	0.268	0.7636	0.2401	0.2294	0.5111
	0.7923	0.6518	0.8435	0.6439	0.589	0.8527

Prewitt, and Roberts obtained lower entropy values indicating that noise and randomness are lower, however it results in true edge information loss overall, see Figure 3(b,d,e). This can also be seen on the loss of major edge details in test images Light Microscopy (A), Lena, Horse, Electric Circuit, and Grape image edge detection results of these methods. Our proposed MSFI obtained entropy values higher than Sobel, Prewitt, and Roberts however compared to Canny, the values are lower indicating meaningful edge detections without much noisy pixels. In particular, compared to Canny, see Figure 3(c) we detected less noisy edge pixels indicating the robustness of our approach, see Figure 3(g). Similar observations can be made for the FoM metric values, and in general, our MSFI obtained better performance overall compared to FI, see Figure 3(f), as can be supported by higher FoM values in across all the test images.

IV. CONCLUSION

In this article, we considered an image edge detection method by combining multiscale gradient maps and Fisher information. A non-parametric and unsupervised edge detection algorithm is proposed with better performance than traditional gradient based edge detectors and a basic Fisher information based edge detector from the literature. Experimental results on a variety of natural is undertaken with PSNR error metric. Overall, the proposed edge detection method obtained better results than other methods in the literature. Future works include incorporating the multiscale gradient maps with other entropies such as the Shannon, Renyi, or adaptive entropy [8] for image thresholding and edge detection.
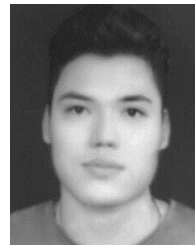
REFERENCES

[1] G. A.Abdel-Azim, S. Abdel-Khalek, and A. S. Obada, "A novel edge detection algorithm for image based on non-parametric Fisher information measure," *Appl. Comput. Math.*, vol. 14, no. 3, pp. 316–327, 2015.

[2] J. Canny, "A computational approach to edge detection," *IEEE Trans. Pattern Anal. Mach. Intell.*, vol. PAMI-8, no. 6, pp. 679–698, Nov. 1986.

[3] R. A. Fisher, "Theory of statistical estimation," *Proc. Cambridge Phil. Soc.*, vol. 22, pp. 700–725, Jul. 1925.

[4] V. B. S. Prasath and R. Delhibabu, "Automatic mucosa detection in video capsule endoscopy with adaptive thresholding," in *Proc. Int. Conf. Comput. Intell. Data Mining*. Cham, Switzerland: Springer, vol. 410, 2015, pp. 95–102.

[5] J. M. S. Prewitt, "Object enhancement and extraction," in *Picture Processing and Psychopictorics*. New York, NY, USA: Academic, 1970, pp. 75–149.

[6] L. G. Roberts, *Machine Perception of Three-Dimensional Solids* (Optical and Electro-Optical Information Processing). Cambridge, MA, USA: MIT Press, 1965, pp. 159–197.

[7] I. E. Sobel, "Camera models and machine perception," Ph.D. dissertation, Dept. Elect. Eng., Stanford Univ., Stanford, CA, USA, Aug. 1970.

[8] V. B. S. Prasath, S. Surineni, K. Gao, G. Seetharaman, and K. Palaniappan, "CSANG: Continuous scale anisotropic Gaussians for robust linear structure extraction," in *Proc. IEEE Appl. Imag. Pattern Recognit. Workshop (AIPR)*, Washington, DC, USA, Oct. 2016, pp. 1–7.

[9] J. Shi, H. Jin, and Z. Xiao, "A novel hybrid edge detection method for polarimetric SAR images," *IEEE Access*, vol. 8, pp. 8974–8991, 2020.

[10] S. Prasath and D. N. Thanh, "Structure tensor adaptive total variation for image restoration," *TURKISH J. Electr. Eng. Comput. Sci.*, vol. 27, no. 2, pp. 1147–1156, Mar. 2019.

[11] Z. Zheng, B. Zha, Y. Xuchen, H. Yuan, Y. Gao, and H. Zhang, "Adaptive edge detection algorithm based on grey entropy theory and textural features," *IEEE Access*, vol. 7, pp. 92943–92954, 2019.

[12] A. Abdullah Yahya, J. Tan, B. Su, K. Liu, and A. N. Hadi, "Image edge detection method based on anisotropic diffusion and total variation models," *J. Eng.*, vol. 2019, no. 2, pp. 455–460, Feb. 2019.

[13] Y. Li, Y. Bi, W. Zhang, and C. Sun, "Multi-scale anisotropic Gaussian kernels for image edge detection," *IEEE Access*, vol. 8, pp. 1803–1812, 2020.

[14] V. B. Surya Prasath, D. Vorotnikov, R. Pelapur, S. Jose, G. Seetharaman, and K. Palaniappan, "Multiscale tikhonov-total variation image restoration using spatially varying edge coherence exponent," *IEEE Trans. Image Process.*, vol. 24, no. 12, pp. 5220–5235, Dec. 2015.

[15] Y. He and L. M. Ni, "A novel scheme based on the diffusion to edge detection," *IEEE Trans. Image Process.*, vol. 28, no. 4, pp. 1613–1624, Apr. 2019.

[16] M. Yildirim and F. Kacar, "Retina-inspired neuromorphic edge enhancing and edge detection," *AEU-Int. J. Electron. Commun.*, vol. 115, Feb. 2020, Art. no. 153038.

[17] L. Wang, Y. Shen, H. Liu, and Z. Guo, "An accurate and efficient multi-category edge detection method," *Cognit. Syst. Res.*, vol. 58, pp. 160–172, Dec. 2019.

[18] N. S. Dagar and P. K. Dahiya, "Edge detection technique using binary particle swarm optimization," *Procedia Comput. Sci.*, vol. 167, pp. 1421–1436, 2020.

[19] Y. Shi, Z. Huo, J. Qin, and Y. Li, "Automatic prior shape selection for image edge detection with modified Mumford–Shah model," *Comput. Math. Appl.*, vol. 79, no. 6, pp. 1644–1660, Mar. 2020.

[20] E. Sert and D. Avci, "A new edge detection approach via neutrosophy based on maximum norm entropy," *Expert Syst. Appl.*, vol. 115, pp. 499–511, Jan. 2019.

[21] S. M. Ismail, L. A. Said, A. G. Radwan, A. H. Madian, and M. F. Abu-ElYazeed, "A novel image encryption system merging fractional-order edge detection and generalized chaotic maps," *Signal Process.*, vol. 167, Feb. 2020, Art. no. 107280.

[22] C. I. Gonzalez, P. Melin, J. R. Castro, O. Castillo, and O. Mendoza, "Optimization of interval type-2 fuzzy systems for image edge detection," *Appl. Soft Comput.*, vol. 47, pp. 631–643, Oct. 2016.

[23] L. Romani, M. Rossini, and D. Schenone, "Edge detection methods based on RBF interpolation," *J. Comput. Appl. Math.*, vol. 349, pp. 532–547, Mar. 2019.

[24] C. I. Gonzalez, P. Melin, J. R. Castro, and O. Castillo, "Edge detection approach based on type-2 fuzzy images," *J. Multiple-Valued Logic Soft Comput.*, vol. 33, nos. 4–5, pp. 431–458, 2019.

[25] S. Yuan, D. Xiang, X. Liu, X. Zhou, and P. Bing, "Edge detection based on computational ghost imaging with structured illuminations," *Opt. Commun.*, vol. 410, pp. 350–355, Mar. 2018.

[26] A. Zotin, K. Simonov, M. Kurako, Y. Hamad, and S. Kirillova, "Edge detection in MRI brain tumor images based on fuzzy C-means clustering," *Procedia Comput. Sci.*, vol. 126, pp. 1261–1270, Jan. 2018.

[27] W. Pratt, *Digital Image Processing*. Hoboken, NJ, USA: Wiley, 1978.

[28] S. Maqsood, U. Javed, M. M. Riaz, M. Muzammil, F. Muhammad, and S. Kim, "Multiscale image matting based multi-focus image fusion technique," *Electronics*, vol. 9, no. 3, p. 472, Mar. 2020.

[29] P. Melin, C. I. Gonzalez, J. R. Castro, O. Mendoza, and O. Castillo, "Edge-detection method for image processing based on generalized type-2 fuzzy logic," *IEEE Trans. Fuzzy Syst.*, vol. 22, no. 6, pp. 1515–1525, Dec. 2014.

[30] D. N. H. Thanh, N. H. Hai, V. B. S. Prasath, L. M. Hieu, and J. M. R. S. Tavares, "A two-stage filter for high density salt and pepper denoising," *Multimedia Tools Appl.*, Apr. 2020, doi: 10.1007/s11042-020-08887-6.

[31] D. N. H. Thanh, V. B. S. Prasath, L. M. Hieu, and S. Dvoenko, "An adaptive method for image restoration based on high-order total variation and inverse gradient," *Signal, Image Video Process.*, Feb. 2020, doi: 10.1007/s11760-020-01657-9.

[32] U. Erkan, S. Enginoğlu, D. N. H. Thanh, and L. M. Hieu, "Adaptive frequency median filter for the salt and pepper denoising problem," *IET Image Process.*, vol. 14, no. 7, pp. 1291–1302, May 2020, doi: 10.1049/iet-ipr.2019.0398.

DANG NGOC HOANG THANH received the bachelor's and M.Sc. degrees in applied mathematics from Belarusian State University, in 2008 and 2009, respectively, and the Ph.D. degree in computer science from Tula State University, Russia, in 2016. He was a Lecturer with the Department of Information Technology, Hue College of Industry, Vietnam. He is currently an Assistant Professor with the Department of Information Technology, School of Business Information Technology, University of Economics Ho Chi Minh City, Vietnam. He has more than 60 works on international peer-reviewed journals and conference proceedings, five book chapters, one book, and one European Patent. His research interests include image processing, computer vision, machine learning, data classification, computational mathematics, fuzzy mathematics, and optimization. He is a member of scientific organization INSTICC, Portugal, ACM, USA, and IAENG, Taiwan. He is also a member of international conferences committee, such as the IEEE ICCE 2018, Vietnam, IWBBIO, Spain, the IEEE ICIEV, USA, the IEEE ICEEE, Turkey, ICIEE, Japan, ICoCTA, Australia, and ICMTEL, U.K.

NGUYEN QUOC HUNG received the Ph.D. degree in computer science from the Hanoi University of Science and Technology (HUST), in 2016. He is currently a Senior Lecturer and a Researcher with the School of Business Information Technology (BIT), University of Economics Ho Chi Minh City (UEH). His research interests include methods for acquiring, processing, analyzing in order to understand images, and human–robot interaction.

V. B. SURYA PRASATH received the Ph.D. degree in mathematics from IIT Madras, Chennai, India, in 2009. He has been an Assistant Professor with the Division of Biomedical Informatics, Cincinnati Children's Hospital Medical Center, and the Departments of Biomedical Informatics, Electrical Engineering, and Computer Science, University of Cincinnati, since 2018. He was a Postdoctoral Fellow with the Department of Mathematics, University of Coimbra, Portugal, for two years, from 2010 to 2011. From 2012 to 2015, he was with the Computational Imaging and VisAnalysis (CIVA) Laboratory, University of Missouri, USA, as a Postdoctoral Fellow, and from 2016 to 2017, as an Assistant Research Professor. He had summer fellowships/visits at Kitware Inc., NY, USA, The Fields Institute, Canada, and IPAM, University of California Los Angeles (UCLA), USA. His main research interests include nonlinear PDEs, regularization methods, inverse and ill-posed problems, variational, PDE-based image processing, and computer vision with applications in remote sensing, and biomedical imaging domains. His current research interests include data science and bioimage informatics with machine learning techniques.

LE MINH HIEU received the bachelor's and M.Sc. degrees in applied mathematics and the Ph.D. degree in computational mathematics from Belarusian State University, in 2009, 2010, and 2018, respectively. He is currently an Assistant Professor with the University of Economics–The University of Danang, Vietnam. He has more than 40 works on international peer-reviewed journals and conference proceedings. His research interests include finite difference schemes, nonlinear PDEs, image processing, machine learning, financial mathematics, and computational mathematics. In 2018, he was awarded a certificate for excellent researchers by the Danang People's Committee.

• • •